Journal of the Australian Ceramic Society (2020) 56:1301–1307
https://doi.org/10.1007/s41779-020-00469-x

RESEARCH

Studies of microstructure and dielectric properties of $CaCu_3Mn_4O_{12}$ complex perovskite oxide synthesized by chemical route

Vinod Kumar[1] · Santosh Pandey[1] · Shruti Singh[1] · Manish KumarVerma[1] · Atendra Kumar[1] · N. B. Singh[2] · K. D. Mandal[1]

Received: 5 December 2019 / Revised: 4 March 2020 / Accepted: 28 April 2020 / Published online: 20 May 2020

Abstract

$CaCu_3Mn_4O_{12}$ (CCMO) ceramic was successfully synthesized by chemical route. The phase formation was to be examined by X-ray diffraction (XRD) pattern of the sintered pellet (850 °C for 6 h), and the crystalline size was found to be 21 nm. Raman shift observed at 3364 to 991 cm^{-1}, clearly confirmed the existence of copper oxide phase at the grain and grain boundaries of the polycrystalline of CCMO complex perovskite oxide. The grain morphology of CCMO ceramic was studied by using HR-SEM, observing the needle-like phase. The particle size observed by TEM measurement was found to be 146.34 nm. The dielectric constant and dielectric loss were found to be 3.3 × 102 and 1.2 respectively.

Keywords Dielectric properties · Chemical route · Raman spectra · Needle-like phase

Introduction

Material having high dielectric permittivity played a very important role in technological application such as capacitor-based components like capacitor, resonator, and other microelectronic devices. The quadruple perovskite materials like $CaCu_3Ti_4O_{12}$ (CCTO) has concerned much attention during last few years due to the great dielectric constant ($\varepsilon' \sim 10^4$) over a wide range of temperature. The CCTO is unlucky that its dielectric loss relatively is very high and also sensitive against radio frequency region, due to this region not suitable for using as capacitor-based based devices. It is well known that tangent loss of ceramic related to the mechanism of internal barrier layer capacitance (IBLC) of dielectric responds well explained by impedance spectroscopy measurement. It was well explained by Sinclair et al. that CCTO ceramic is electrically homogeneous and contains semiconducting grain and grain boundary. It is responsible for high dielectric constant due to internal layer barrier capacitance [1–4]. The CCTO and CCMO both are analogous to each in crystal structure. In a previous report, the CCMO was synthesized through Sol-gel synthesis, and the drawback of this method is that larger number of secondary peaks is recorded [5].

In this work, $CaCu_3Mn_4O_{12}$ has been successfully synthesized through the chemical route. The chemical route has more advance due time, sintering temperature point of view of CCMO ceramic. The chemical route is very easy to reach more purity at the ionic level of CCMO ceramic. The advantage of chemical route is more significant saving of time and energy consumption compared with traditional methods such as sol-gel technique. The chemical route, working to obtain better powder characteristics, more homogeneity, and fine particle size range, impacts the structure of the material. The dielectric properties and insulating grains and grain boundaries of the CCMO ceramic were studied and observed.

Synthesis of material

In this present work, CCMO ceramic was synthesized by the chemical route. In this method, metal nitrates were taken in stoichiometric amount $Ca(NO_3)_2.4H_2O$ (98% Merck, India), $Cu(NO_3)_2.6H_2O$ (Pure 99% Merck, India), and $C_4H_4MnO_4.H_2O$ (Aldrich 99% Pure). All metal nitrates and manganese acetate were mixed in the required amount of distilled water, and glycine was counter as the chelating agent

✉ K. D. Mandal
kdmandal.apc@itbhu.ac.in

[1] Department of Chemistry, Indian Institute of Technology (Banaras Hindu University), Varanasi, Uttar Pradesh 221005, India

[2] Department of Chemistry &Biochemistry, University of Maryland, Baltimore Country, 1000 Hilltop Circle, Baltimore, MD 21250, USA

which is equivalent amount to the metal ions mixed with the solution. In a beaker, these metal nitrate solution mixtures were magnetically stirred on the plate and the temperature was slowly increased to 70–80 °C and was kept on for 12 to 15 h to remove excess water and accelerate polyesterification. CCMO was black. Then, CCMO was well-crystallized into powders and ground using mortar and pestle, and sintered at 850 °C for 6 h in a muffle furnace before pelletization. Cylindrical pellets were prepared using polyvinyl alcohol (PVA 2 wt%) used as a binder with calcined powders by hydraulic press, applying pressure of 4 to 5 tons for 2 min. The binder was burnt out at 500 °C for 2 h. The sample was characterized by XRD, Raman spectra, high-resolution scanning electron microscopy (HR-SEM), energy dispersive X-ray spectra (EDX), and dielectric measurement.

Results and discussion

X-ray diffraction analysis

Figure 1 a shows the X-ray diffraction (XRD) pattern of CCMO ceramic sintered 850 °C for 6 h on scan rate 2 degree per minute. The phase formation of CCMO ceramic confirms with the help of JCPDS card no. 75-2188, and some impurity of copper oxide (CuO) is also observed in the XRD pattern indexed on the basis of the JCPDS card no. 45-0937 [1]. The peak position of CCMO obtained at 29.57°, 34.45°, 38.47°, 49.38°, and 61.45° was found to be very sharp in the XRD pattern. However, very small intense peak is observed at 38.47°, 49.38°, and 61.45°. The peak appears like that in the $CaCu_3Ti_4O_{12}$ phase [6]. The crystallite size (D) of CCMO ceramic was calculated by using Debye Scherer's formula.

$$D = \frac{k\lambda}{\beta \mathrm{Cos}\ \theta} \tag{1}$$

In the above Eq. (1), k is the crystal shape coefficient (k = 0.89), λ is the wavelength (1.54 Å) of the X-ray, β is the full width at half maximum (FWHM), and θ is Bragg's diffraction angle. The value of crystallite size obtained for CCMO ceramic was found to be 21 nm.

Figure 1 b depicts Retvield refinement of the XRD pattern was carried out for phase confirmation and crystal structure of the $CaCu_3Mn_4O_{12}$ (CCMO) material sintered at 830 °C for 6 h, which emphasize the cubic structure (space group—$I\,m\,3$) for CCMO ceramic along with the minor impurity of the copper oxide (CuO) having monoclinic structure. The refined lattice parameter observed after refinement is summarized in Table 1. It is clear from the figure that the calculated pattern (red color) is exactly lie on the observed pattern (black line) indicating good fitting of the XRD pattern and goodness of fit also confirms by the help of lower value of χ^2. The obtained results confirm the phase formation of CCMO ceramic with no changes during the process of refinement [7].

Raman studies

Figure 2 displays the Raman spectra of CCMO ceramic sintered at 850 °C for 6 h. The highest intensity peak and lowest intensity peak positions are observed at 785 cm^{-1} and 324 cm^{-1} which conforms the phase formation of CCMO

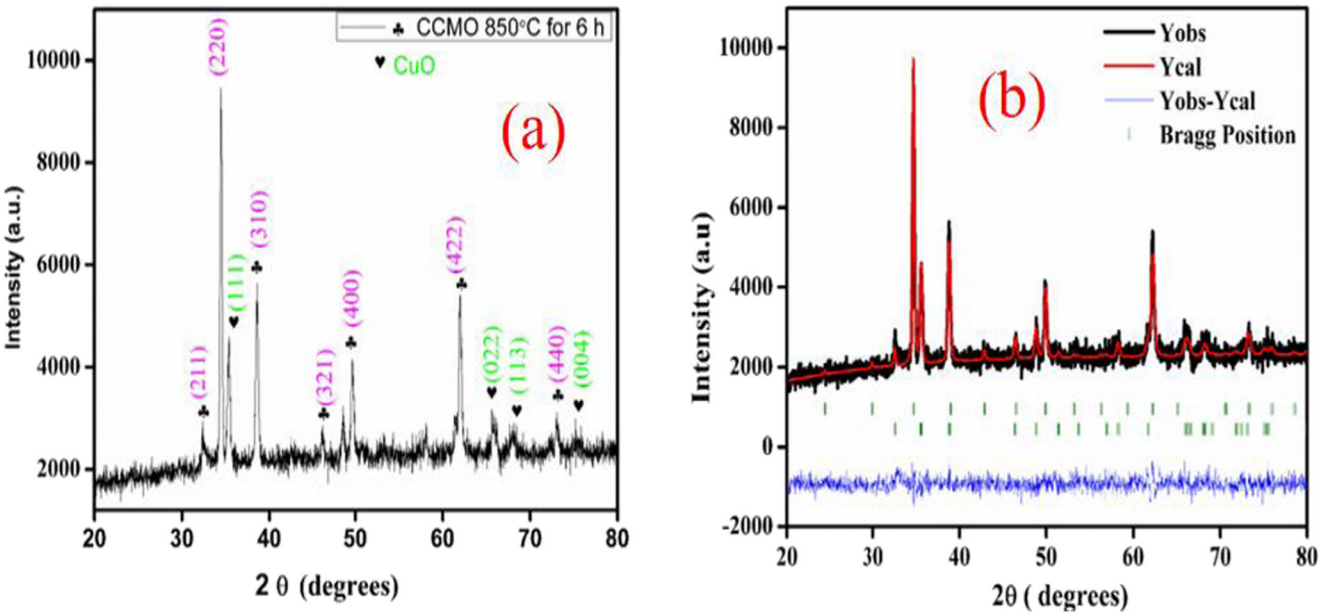

Fig. 1 **a** X-ray diffraction pattern of CCMO ceramic and **b** Retvield refinement of the XRD pattern sintered at 850 °C 6 h

Table 1 Refined structural parameters of CCMO ceramic

$\chi^2 = 5.10$		
Phase 1	$CaCu_3Mn_4O_{12}$ (CCMO)	Space group—$I\,m\,\bar{3}$
Cell parameters	$a = b = c = 7.307762$ Å	Angle $\alpha = \beta = \gamma = 90°$
Bragg *R*-factor	4.183	
RF-factor	4.26	
Phase 2	CuO (copper oxide)	Space group—$C\,1\,2/c\,1$
Cell parameters	a = 4.689756 Å, $b = 3.414203$ Å, $c = 5.128606$ Å	Angle $\alpha = \gamma = 90°$, $\beta = 99.418$
Bragg *R*-factor	3.477	
RF-factor	2.481	

ceramic. The lowest intensity peak observed at 324 cm^{-1} is evidently support the existence of CuO at the grain boundary [8, 9]. In Raman spectra, which displays the graph, there are minor peaks observed in both the lowest intensity and highest intensity; the peak positions are at the 324 cm^{-1}, 376 cm^{-1}, 528 cm^{-1}, 599 cm^{-1}, 743 cm^{-1}, 785 cm^{-1}, 918 cm^{-1}, and 991 cm^{-1}.The above peak 324 cm^{-1} evidently shows and relates to the Eg 528 cm^{-1}, and 599 cm^{-1} peak is associated with the A_1g symmetry octahedral MnO_6 rotation and peak observed at 599 cm^{-1} with Fg symmetry (Mn–O–Mn) anti-stretching. The peak with the highest intensity displaying at the position743 cm^{-1} could be related to the first principle calculation, at 785 cm^{-1}, this peak could be represented to the existing symmetrical stretching breathing of MnO [10, 11]. The low-intensity peak observed at the position 324 cm^{-1}, 376 cm^{-1} and 918 cm^{-1}, 991 cm^{-1}, out of evidently two may be at first two not be expectable to the CCMO phase to the CCMO structure model, represent to the minor phase of CuO and MnO [12, 13]. In the CCMO ceramic, the peak observed at 324 cm^{-1} intensity represents to the grain boundary and supplementary peak; it was also to be noted that

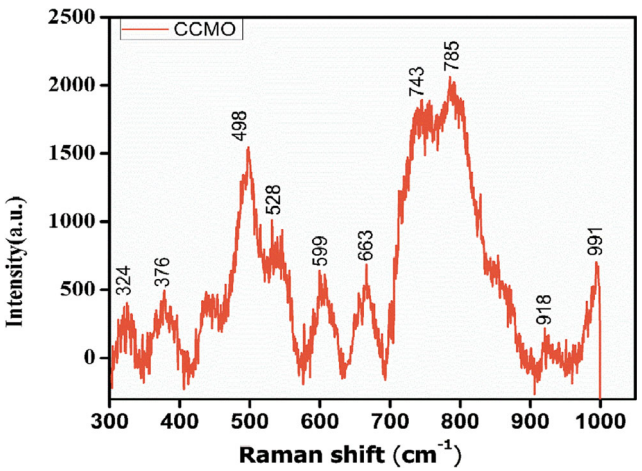

Fig. 2 Raman spectra of $CaCu_3Mn_4O_{12}$ perovskite oxides sintered at 850 °C for 6 h

376 cm^{-1} and 599 cm^{-1} peaks were not found at the grain of CCMO. The peak intensity 376 cm^{-1} is associated with Raman spectral line and justified the presence CuO in the grain boundary of CCMO ceramic and its active Raman mode A_2g which was already reported [2].

High-resolution scanning electron microscopic studies

Figure 3 a shows the microstructure of CCMO ceramic sintered at 850 °C for 6 h. The average grain size is observed in the range of 0.79 μm. The microstructure of CCMO ceramic was looking uniformly needle-like phase obtained in the sintered complex perovskite oxide [14]. The morphology of CCMO ceramic sintered at 850 °C for 6 h, also displaying the dense arrangement in the needle-like phase grain structure [15]. The uniformity of grain formation will support the microstructural densification that will benefit in the electrical and dielectric properties. In a previous report [4], the grain size morphology of CCMO ceramic sintered at 700 °C for 18-h dwelling time is the best sintering parameter for the chemical route synthesis of CCMO ceramic and 850 °C for 6 h that causes better parameters than those of other sintering parameter Sol-gel methods [3, 16, 17].

Energy dispersive X-ray spectra analysis

Figure 3 b and c display the spectrum and table of stoichiometry of CCMO ceramic sintered at 850 °C for 8 h. Investigations of the result evidently confirm the presence of Ca, Cu, Mn, and O as per stoichiometric ratio in the CCMO ceramics, with an extra peak of 2.15 k eV. Pt coating was performed by ion beam sputtering for increasing the conductivity, which was necessary to avoid charging of samples. The EDX results confirmed the existence of individual element in the ceramic. The quantitative analysis is shown in the spectrum that atomic percentages of the elements for Ca, Cu, Mn, and oxygen were observed to be 8.51, 8.94, 26.69, and 55.86 respectively shown in the spectrum.

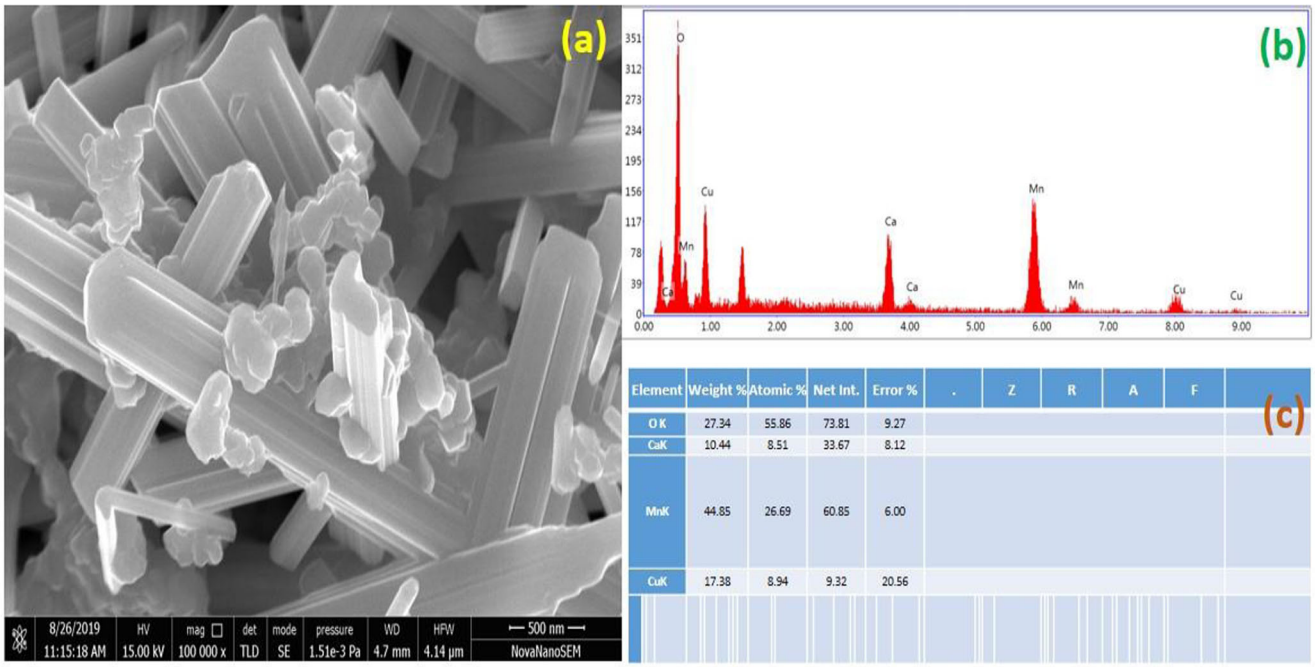

Fig. 3 **a** HR-SEM of CCMO ceramic sintered at 850 °C for 6 h. **b**, **c** Energy dispersive X-ray spectrum of CCMO ceramic with the quantitative elemental percentage

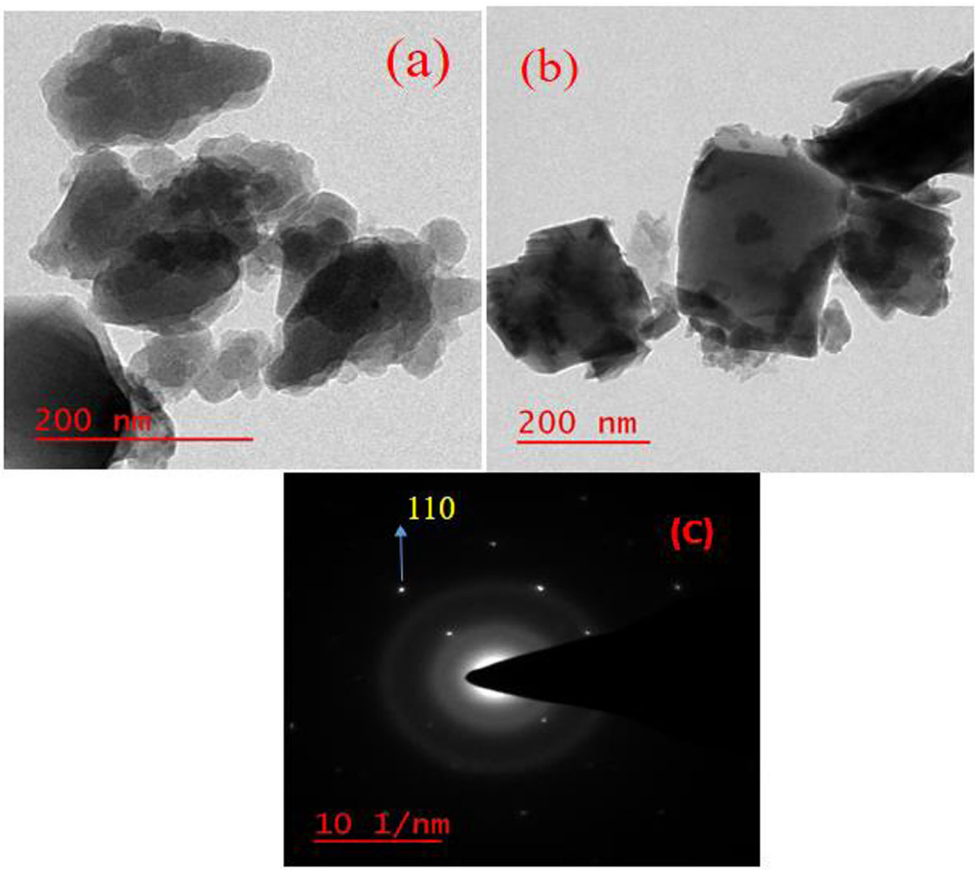

Fig. 4 **a** and **b** indicate bright field TEM image, **c** slected area diffraction (SAED) pattern of CCMO ceramic

High-resolution transmission electron microscopy

Figure 4 a and b indicate the sintered CCMO 850 °C for 8 h. The presence of predominant cubical and spherical shape of the particle is noted. The particle size measured by TEM instrument is noted that it shows the crystalline nature of the CCMO ceramic. Figure 5 c indicates the selected area electron diffraction (SAED) patterns show the parallel spots which confirm the presence normal peak of CCMO. It is explained by the SEAD pattern that the ring-like spots are indexed trough on the basis of basic of CCTO body-centered cubic (BCC) perovskite structure resemble with CCTO ceramic which data also supported by XRD with JCPDS card no. 34-0097. These spots retain two different planes indexed with the plane (1 1 0) which is also described through TEM that the particle size of CCMO 146.34 nm which is supported to that in nanocrystalline range and also supported by SEM and XRD data.

Dielectric studies

Figure 4 a and b display the variation of dielectric constant and tangent loss of CCMO ceramic with the temperature and few

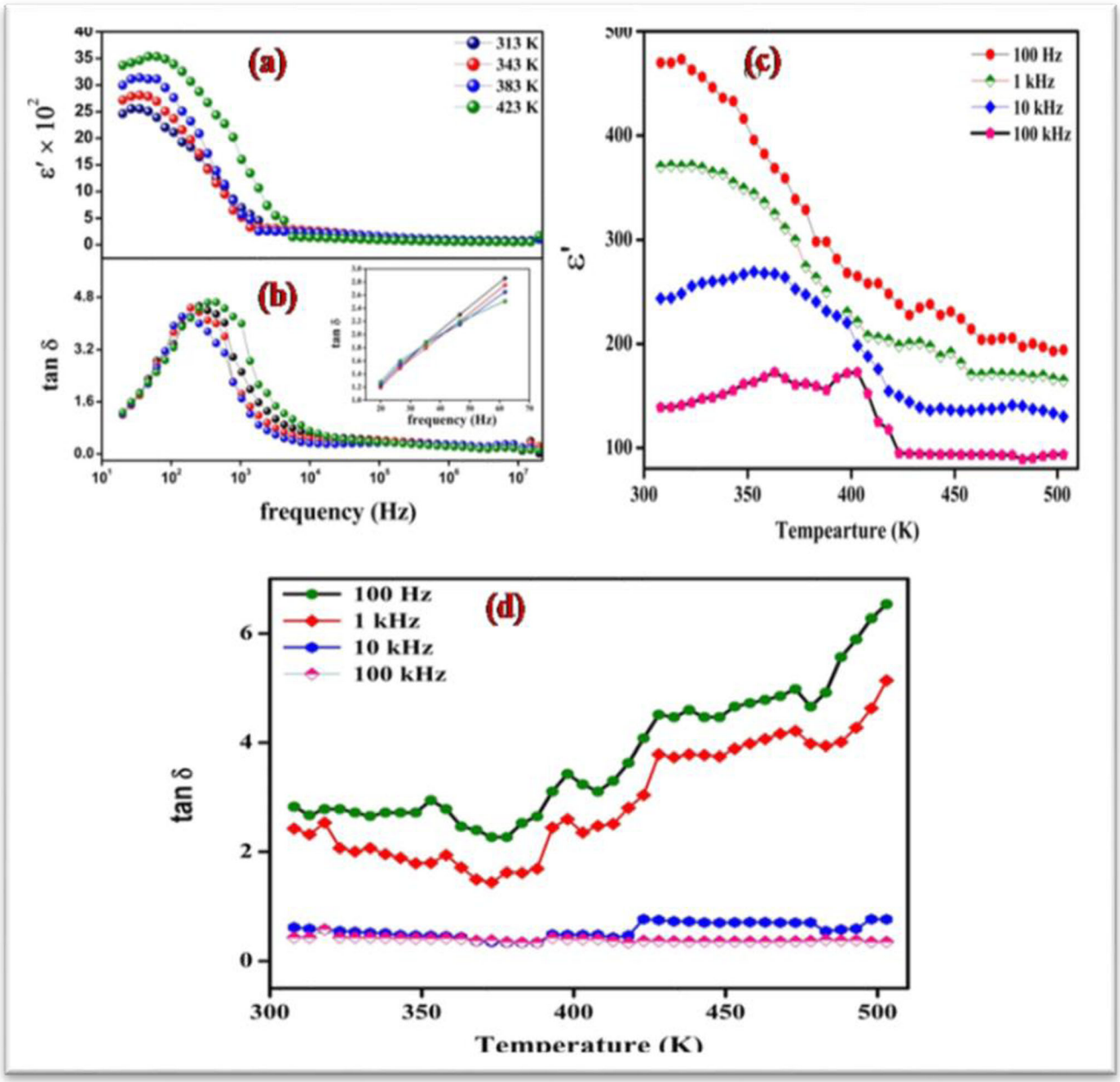

Fig. 5 **a**, **b** Dielectric constant, the tangent loss against frequencies of CCMO ceramic; **c**, **d** tangent loss against temperature at few selected frequencies

selected frequency, respectively. It was to be observed from the plotted graph that the dielectric constant shows temperature-independent 400 to 500 K all measured frequency (100 Hz, 1 kHz,10 kHz, 100 kHz). It is observed from the plotted graph that the broad peak of dielectric constant was to be measured at around 423 K of all measured frequencies. It was to be observed that the dielectric constant decreases by increasing frequency.

Figure 4 c and d display the dielectric constant and tangent loss against temperature of CCMO ceramic. The dielectric constant was to be recorded around 470, 370, 260, and 150 at 100 Hz, 1 kHz, 10 KHz, and 100 kHz at few selected frequencies. The broad peak of dielectric constant and dielectric loss of CCMO ceramic is due caused by oxygen vacancy created during the sintering process, not by the relaxation process [18]. The decreasing in the value of dielectric constant with frequency may be due to space charge polarization. The oxygen vacancy during the sintering process is mainly due to the ceramic oxide material space charge polarization which mainly responds to external electric field. The charges have moved to longer distances in the materials at low frequency so a high dielectric constant was observed, while at high frequency, the space charge polarization no longer follows, so a low dielectric constant was observed.

Conclusions

The $CaCu_3Mn_4O_{12}$ (CCMO) ceramic has successfully synthesized through the chemical route. The phase formation of the ceramic was confirmed by the X-ray diffraction pattern of sintered pellet at lower sintering temperature under atmospheric conditions. The crystalline size of CCMO ceramic was found to be 21 nm. The CCMO ceramic was examined by Raman spectra, and Raman shift of the highest and lowest intensity peak was found to be 785 cm^{-1} and 743 cm^{-1}, and 324 cm^{-1} and 376 cm^{-1} peaks. The microstructural of CCMO ceramic was studied by high-resolution transmission electron microscopy (HR-TEM) and HR-SEM. The elemental composition was examined by the energy-dispersive X-ray spectra. The average grain size of CCMO ceramic with needle-like structure was found to be 0.79 μm. The elemental composition was confirmed by EDX. The particle size was found to be 146.34 nm. The value of dielectric constant and dielectric loss was found to be 3.3×10^2 and 1.2 at 10 Hz, respectively.

Acknowledgments The authors are grateful to the In-charge, CIFC, IIT (BHU) Varanasi, for providing SEM with EDX, Raman facilities.

Funding information Vinod Kumar thanks the Head, Department of Chemistry, and IIT (BHU) Varanasi, India, for providing financial assistance as teaching assistantship.

References

1. Mohammadi, M., Alizadeh, P., Clemens, F.J.: Effect of SiO2 on sintering and dielectric properties of CaCu3Ti4O12 nanofibers. J Alloys Compd. **688**, 270–279 (2016). https://doi.org/10.1016/j.jallcom.2016.06.245
2. Singh, L., Kim, I.W., Sin, B.C., Mandal, K.D., Rai, U.S., Ullah, A., Chung, H., Lee, Y.: Dielectric studies of a nano-crystalline CaCu $_{2.90}$ Zn $_{0.10}$ Ti $_4$ O $_{12}$ electro-ceramic by one pot glycine assisted synthesis from inexpensive TiO $_2$ for energy storage capacitors. RSC AdvRSC Adv. **4**, 52770–52784 (2014). https://doi.org/10.1039/C4RA08915D
3. Nurulhuda, A., Warikh, A.R.M., Hafizzal, Y.: Sol gel synthesis and characterization studies of Cupromanganite CaCu3Mn4O12. IOP Conference Series: Materials Science and Engineering. **226**, 012154 (2017). https://doi.org/10.1088/1757-899X/226/1/012154
4. Kim, C.H., Jang, Y.H., Seo, S.J., Song, C.H., Son, J.Y., Yang, Y.S., Cho, J.H.: Effect of Mn doping on the temperature-dependent anomalous giant dielectric behavior of CaCu 3 Ti 4 O 12. Phys Rev B. **85**, 245210 (2012). https://doi.org/10.1103/PhysRevB.85.245210
5. Vangchangyia, S., Swatsitang, E., Thongbai, P., Pinitsoontorn, S., Yamwong, T., Maensiri, S., Amornkitbamrung, V., Chindaprasirt, P.: Very low loss tangent and high dielectric permittivity in pure-CaCu3Ti4O12 ceramics prepared by a modified sol-gel process. J Am Ceram Soc. **95**, 1497–1500 (2012). https://doi.org/10.1111/j.1551-2916.2012.05147.x
6. Wolska, E., Stempin, K., Krasnowska-Hobbs, O.: X-ray diffraction study on the distribution of lithium ions in LiMn2O4/LiFe5O8 spinel solid solutions. Solid State Ionics. **101–103**, 527–531 (1997). https://doi.org/10.1016/S0167-2738(97)84078-7
7. Structural and electronic transformations in quadruple iron perovskite Ca1−xSrxCu3Fe4O12 - ScienceDirect. 2019. https://www.sciencedirect.com/science/article/pii/S2187076417300246. Accessed Nov 23
8. Yadav, A.K., Singh, P.: A review of the structures of oxide glasses by Raman spectroscopy. RSC Adv. **5**, 67583–67609 (2015). https://doi.org/10.1039/C5RA13043C
9. Influence of thermal annealing on microstructural, morphological, optical properties and surface electronic structure of copper oxide thin films. 2014. Materials Chemistry and Physics 147. Elsevier: 987–995. https://doi.org/10.1016/j.matchemphys.2014.06.047
10. Romero, J.J., Leret, P., Rubio-Marcos, F., Quesada, A., Fernández, J.F.: Evolution of the intergranular phase during sintering of CaCu3Ti4O12 ceramics. J Eur Ceram Soc. **30**, 737–742 (2010). https://doi.org/10.1016/j.jeurceramsoc.2009.08.024
11. Frank, O., Zukalova, M., Laskova, B., Kürti, J., Koltai, J., Kavan, L.: Raman spectra of titanium dioxide (anatase, rutile) with identified oxygen isotopes (16, 17, 18). Phys Chem Chem Phys. **14**, 14567–14572 (2012). https://doi.org/10.1039/C2CP42763J
12. Chen, K., Wu, Y., Liao, J., Liao, J., Zhu, J.: Raman and dielectric spectra of CaCu3Ti3.9O12 ceramics. Integr Ferroelectr. **97**, 143–150 (2008). https://doi.org/10.1080/10584580802089023
13. Huang, X., Zhang, H., Lai, Y., Li, J.: The lowered dielectric loss tangent and grain boundary effects in fluorine-doped calcium copper titanate ceramics. Applied Physics A. **123**, 317 (2017). https://doi.org/10.1007/s00339-017-0947-9
14. Molina-García, A., Miguel, Rees, N.V.: Effect of catalyst carbon supports on the oxygen reduction reaction in alkaline media: a comparative study. RSC Adv. **6**, 94669–94681 (2016). https://doi.org/10.1039/C6RA18894J
15. Nautiyal, A., Autret, C., Honstettre, C., De Almeida-Didry, S., El Amrani, M., Roger, S., Negulescu, B., Ruyter, A.: Local analysis of the grain and grain boundary contributions to the bulk dielectric properties of Ca(cu 3−y mg y)Ti 4 O 12 ceramics: importance of

the potential barrier at the grain boundary. J Eur Ceram Soc. **36**, 1391–1398 (2016). https://doi.org/10.1016/j.jeurceramsoc.2015.12.035

16. Chenavas, J., Joubert, J.C., Marezio, M., Bochu, B.: The synthesis and crystal structure of CaCu3Mn4O12: a new ferromagnetic-perovskite-like compound. J Solid State Chem. **14**, 25–32 (1975). https://doi.org/10.1016/0022-4596(75)90358-8
17. Jumpatam, J., Putasaeng, B., Chanlek, N., Kidkhunthod, P., Thongbai, P., Maensiri, S., Chindaprasirt, P.: Improved giant dielectric properties of CaCu 3 Ti 4 O 12 via simultaneously tuning the electrical properties of grains and grain boundaries by F − substitution. RSC Adv. **7**, 4092–4101 (2017). https://doi.org/10.1039/C6RA27381E
18. Gautam, P., Khare, A., Sunita, S., Singh, N.B., Mandal, K.D.: Characterization of Bi2/3Cu3Ti4O12 ceramics synthesized by semi-wet route. Progress in Natural Science: Materials International. **26**, 567–571 (2016). https://doi.org/10.1016/j.pnsc.2016.11.008